10.1071/WF21135
International Journal of Wildland Fire

Supplementary Material

GAMBUT field experiment of peatland wildfires in Sumatra: from ignition to spread and suppression

Muhammad A. Santoso[A,E], *Eirik G. Christensen*[A], *Hafiz M. F. Amin*[A,B], *Pither Palamba*[C], *Yuqi Hu*[A,D], *Dwi M. J. Purnomo*[A], *Wuquan Cui*[A], *Agus Pamitran*[E], *Franz Richter*[A], *Thomas E. L. Smith*[F], *Yulianto S. Nugroho*[E] and *Guillermo Rein*[A,*]

[A]Department of Mechanical Engineering, and Leverhulme Centre for Wildfires, Environment and Society, Imperial College London, London, SW7 2AZ, UK

[B]School of Computing, Engineering & Digital Technologies, Teesside University, Middlesbrough, UK

[C]Department of Mechanical Engineering, Universitas Cenderawasih, Jayapura, Indonesia

[D]Sichuan Fire Research Institute of the Ministry of Emergency Management, Chengdu, China

[E]Department of Mechanical Engineering, Universitas Indonesia, 16424, West Java, Indonesia

[F]Department of Geography & Environment, London School of Economics & Political Science, London, UK

*Correspondence to: Email: g.rein@imperial.ac.uk

Appendix

Figure A1. Different surface treatment between Plot 1 where surface litter vegetation was left, and Plot 2 and 3 where surface litter vegetation was removed from the plots.

Local survey on the plot topography were conducted by taking the distance from a predetermined height to the surface of the plots (Figure A2A). Figure A2B to D show the topography of the experimental plots showing a significant elevation difference of ~1 m between south and north sides. This topography difference influences the decision on pre-experiment sampling location to investigate the peat properties and on the location of ignition (Figure 4a and b).

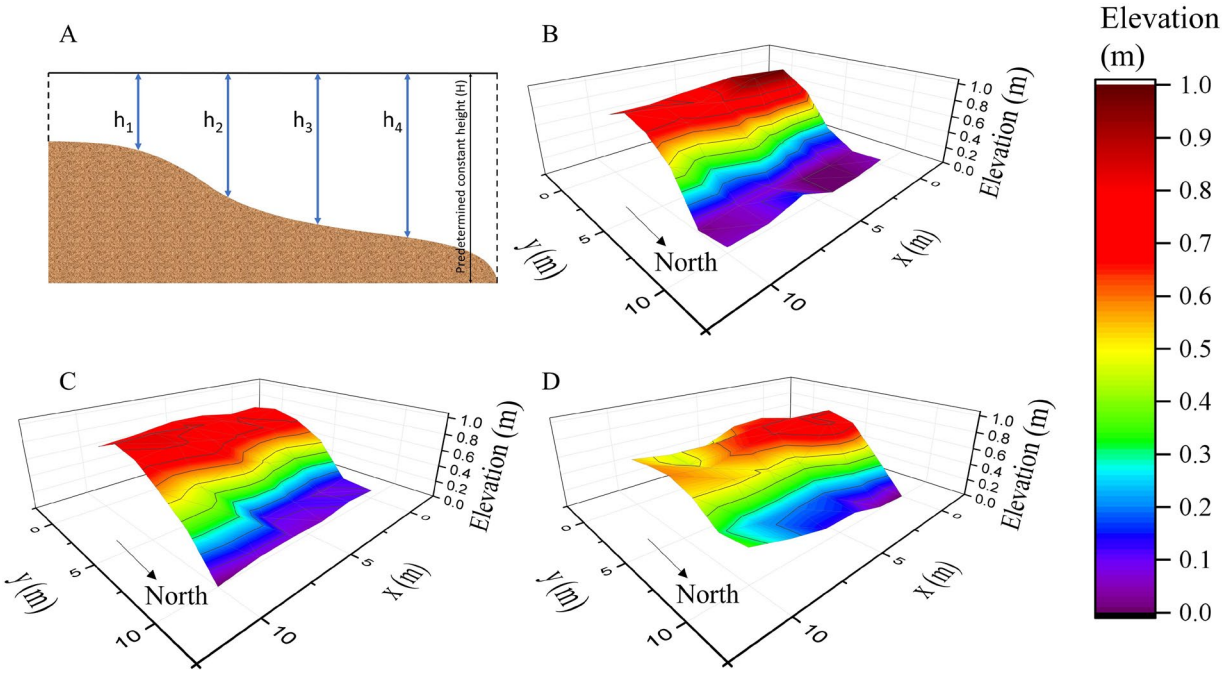

Figure A2. Plot topography measurement. (A) Schematic of the in-situ measurement. Topography of (B) plot 1 (C) plot 2 (D) plot 3

At each point, thermocouples were inserted at an angle using a thermocouple inserter (Figure A3B). This insertion method assumes that smouldering propagation is coming from the right-hand side of Figure A3A. This insertion angle facilitates the thermocouple junctions to be at the predetermined depths, i.e. 10 cm and 30 cm, and records temperature while keeping the thermocouple wire away from the heat and prevents it from melting.

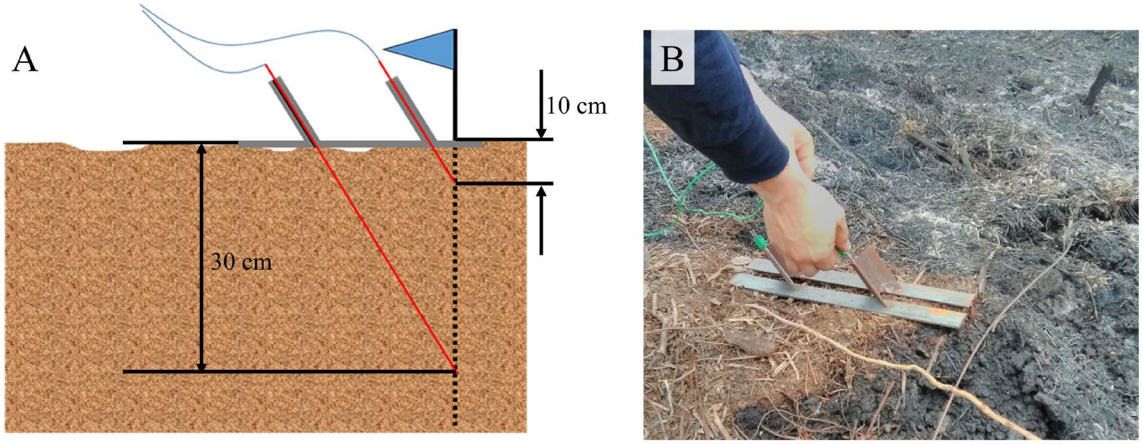

Figure A3. Thermocouple placement (A) Illustration of the insertion of the thermocouples at an angle. Blue flag represents the thermocouple point. (B) thermocouples being inserted during the experiments.

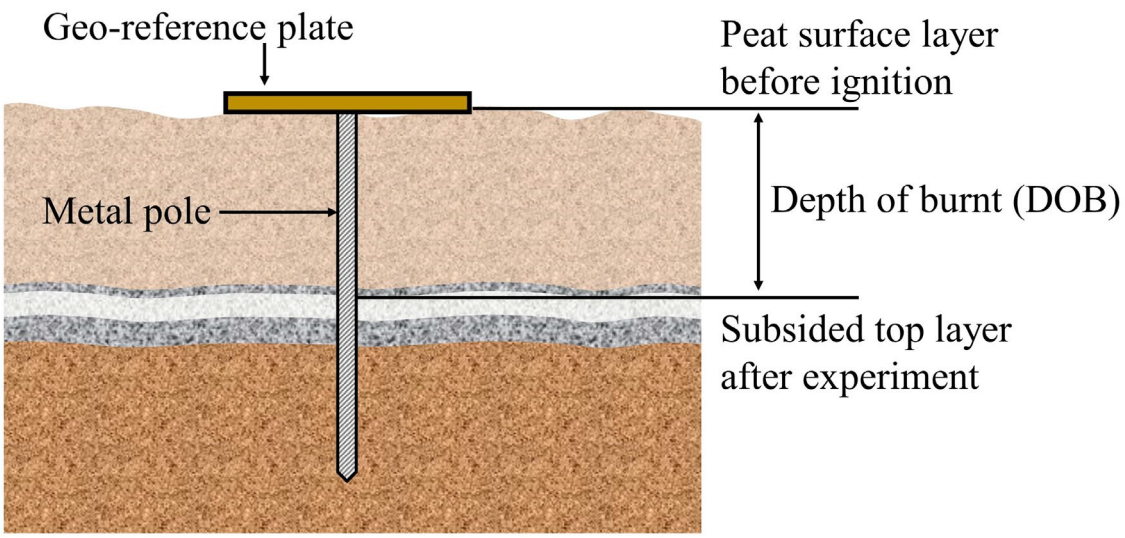

Figure A4. Schematic of the depth of burnt (DOB) measurement

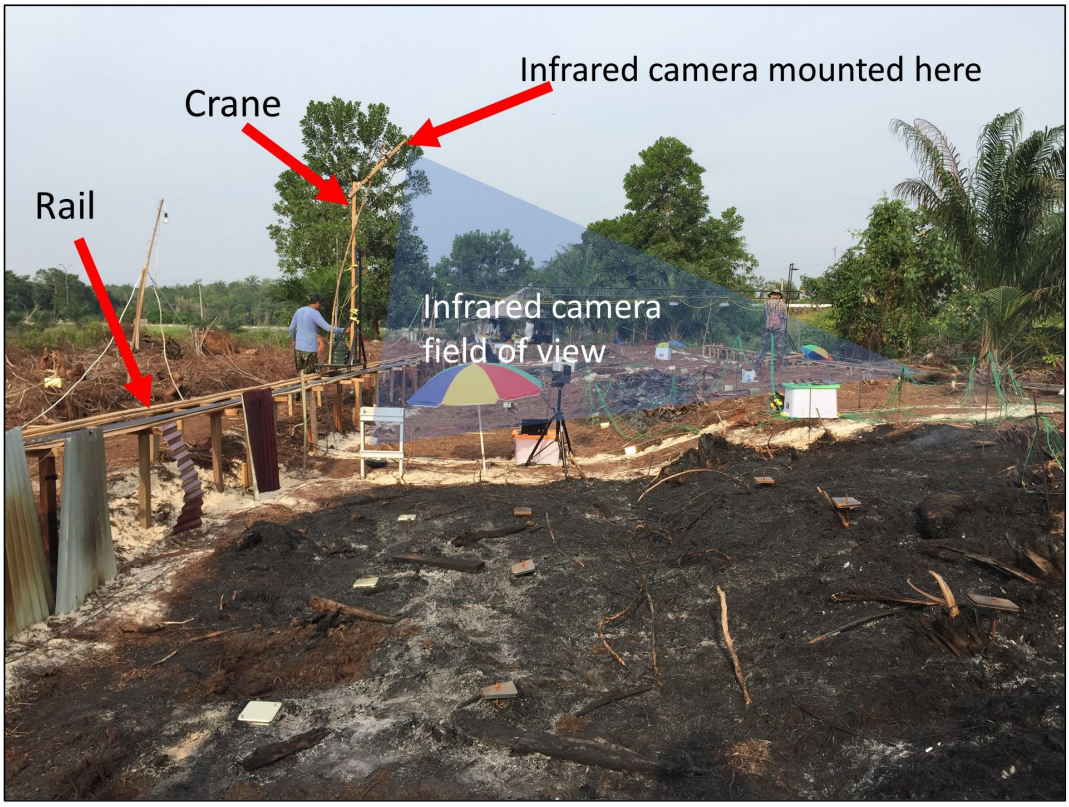

Figure A5. Photo of the crane and rail in the process of capturing smouldering infrared images during the field experiment.

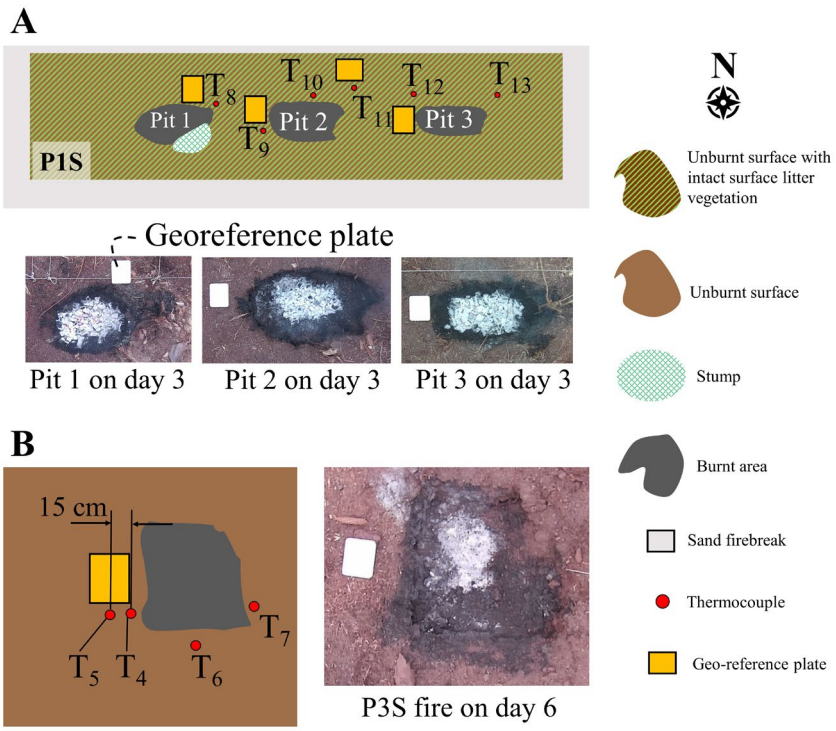

Figure A6. Thermocouple locations in (A) P1S (top image is sketch and bottom images are aerial photographs) and (B) P3S (left image is sketch and right image is an aerial photograph). The geo-reference plate dimension is 0.17×0.14 m^2.

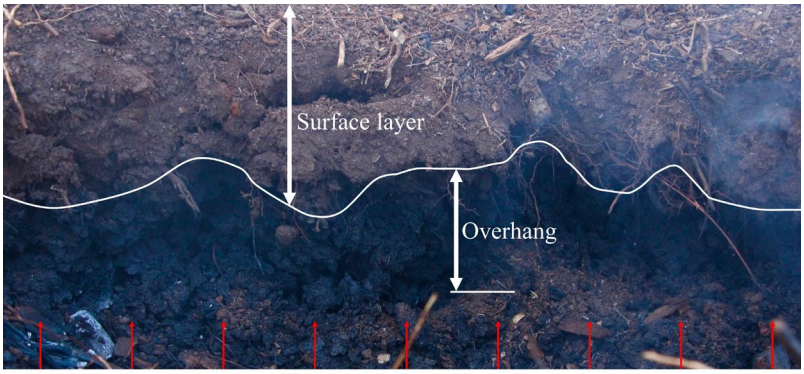

Figure A7. Overhang formation and collapse in this study. In addition to the different spread rate between surface and in-depth layers, the surface vegetation layer provided temporary stability support for overhang formation due to the fibrous structure (photograph by Wuquan Cui).

Smouldering in P1N was self-sustained until day 11 (D11), however temperatures after day 8 (D8) are not reported in this figure due to unclear smouldering propagation because of power cut on the night of day 8 (D8) to the early morning of day 9 (D9) due to a technical issue and on the night of day 9 (D9) to the early morning of day 11 (D11) due to heavy rain on the night of day 9 (D9) (Figure 3b) causing the tent protecting the electrical sources to the measurement devices collapsed, cutting off power supply to data loggers. Figure A8 shows the temperatures in P1N up to day 11 (D11) where technical issue and power cut are indicated by blank temperature data. These occurrences represent the difficulty of conducting smouldering field experiment in peatland forest where harsh environment and logistics management can be challenging.

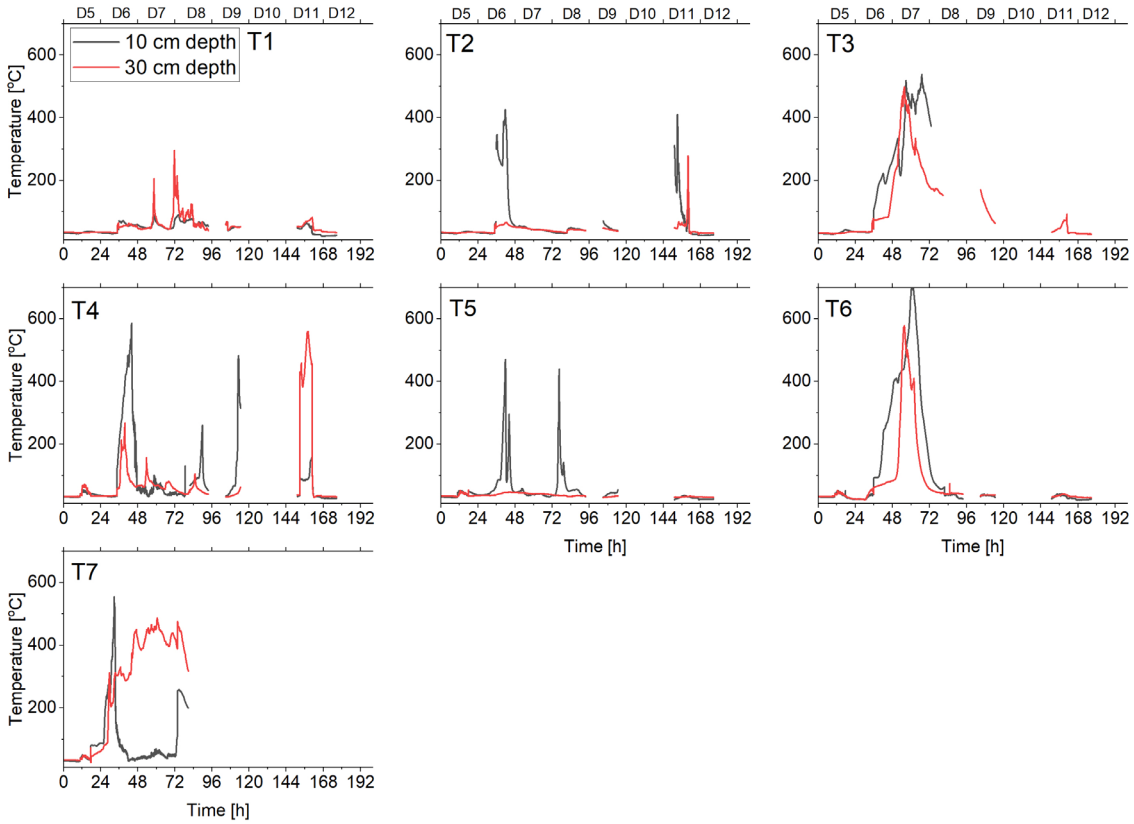

Figure A8. Temperature profiles in P1N fire showing all temperature measurement points as shown in Figure 8a. Time at 0 h indicates 00:00:00 am on day (D5). Day is abbreviated to 'D' in this figure. Slash-and-burn ignition was conducted on day 5 (D5) at ~11:27:00.

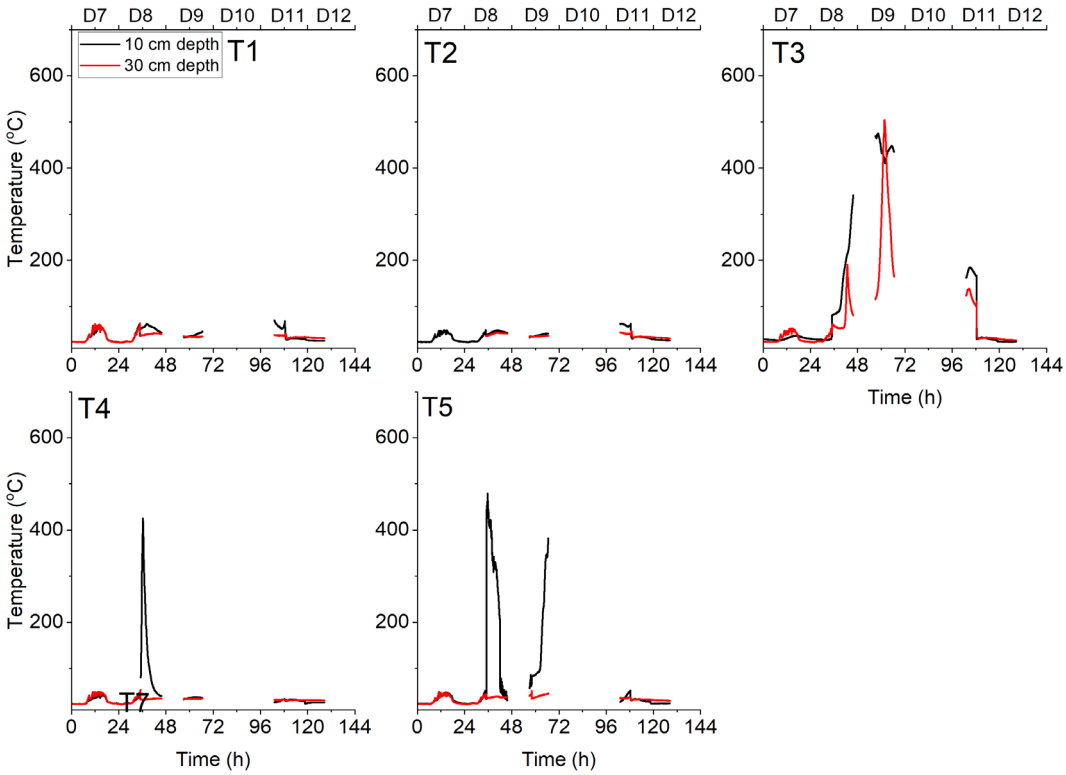

Figure A9. Temperature profiles in P2N fire showing all temperature measurement points as shown in Figure 8b. Time at 0 h indicates 00:00:00 am on day 7 (D7). Day is abbreviated to 'D' in this figure. Slash-and-burn ignition was conducted on day 7 (D7) at ~12:40:00.

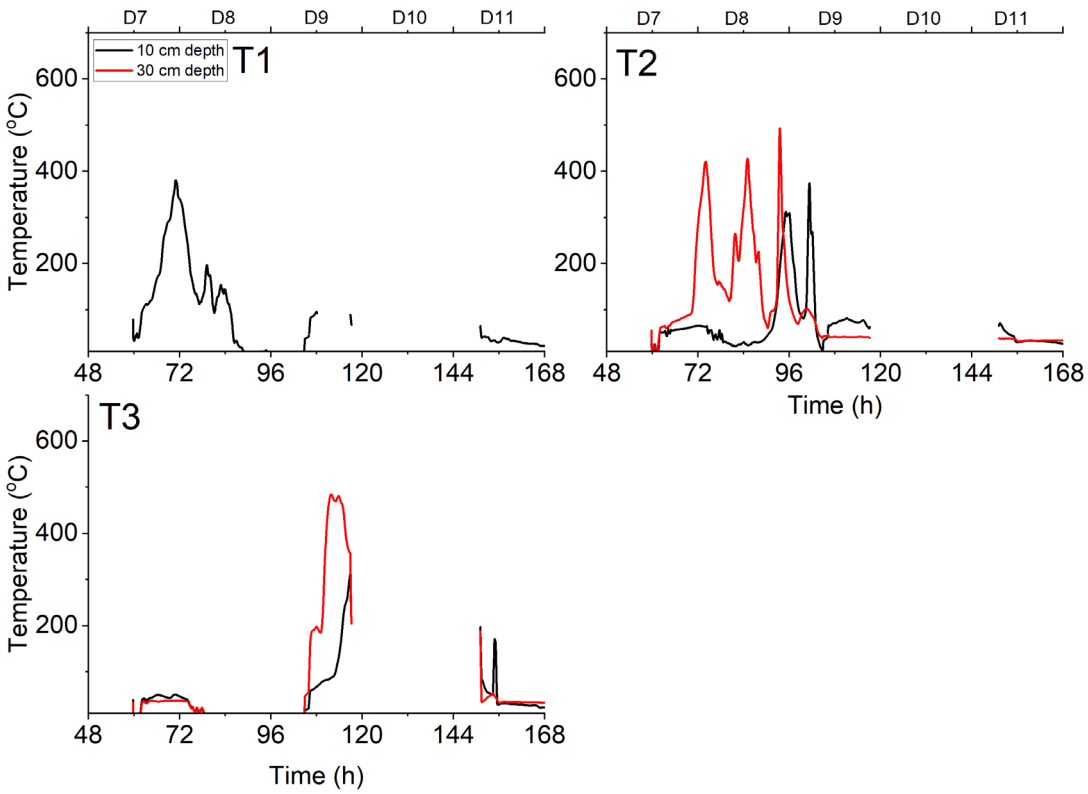

Figure A10. Temperature profiles in P3N fire showing all temperature measurement points as shown in Figure 8c. Time at 48 h indicates 00:00:00 am on day 7 (D7). Day is abbreviated to 'D' in this figure. Slash-and-burn ignition was conducted on day 5 (D5) at ~16:12:00.

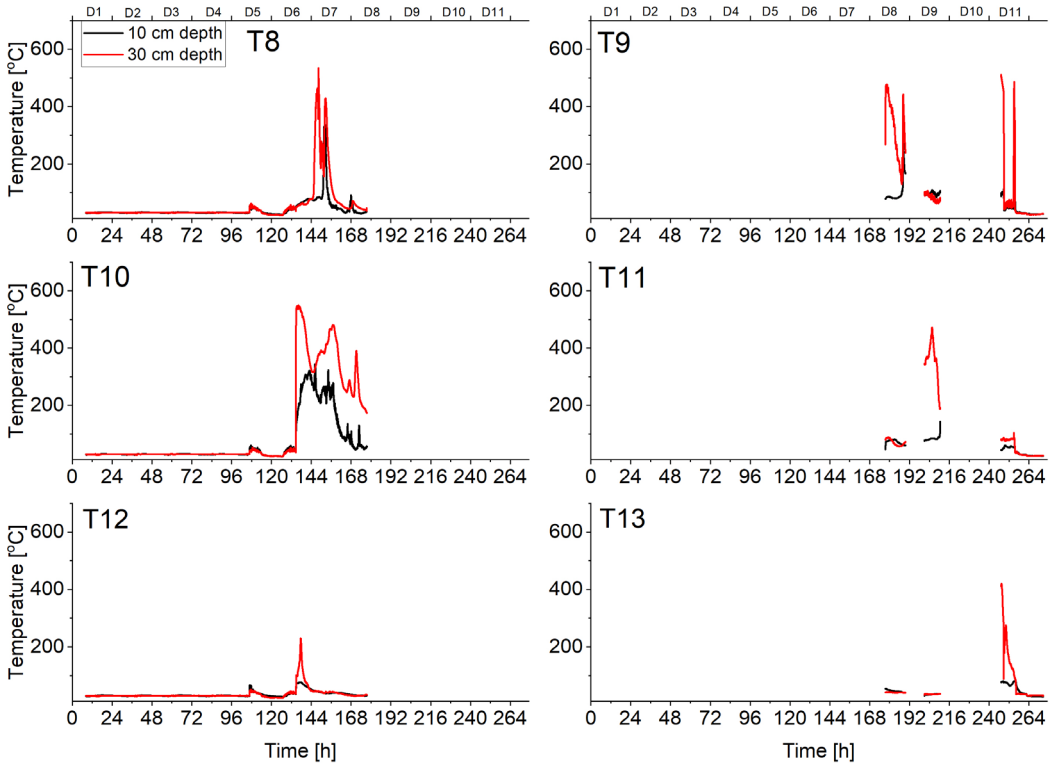

Figure A11. Temperature profiles in P1S fire showing all temperature measurement points as shown in A6A. Time at 0 h indicates 00:00:00 am on day 1 (D1). Day is abbreviated to 'D' in this figure. Embers ignition was conducted on day 1 (D1) at ~12:00:00.

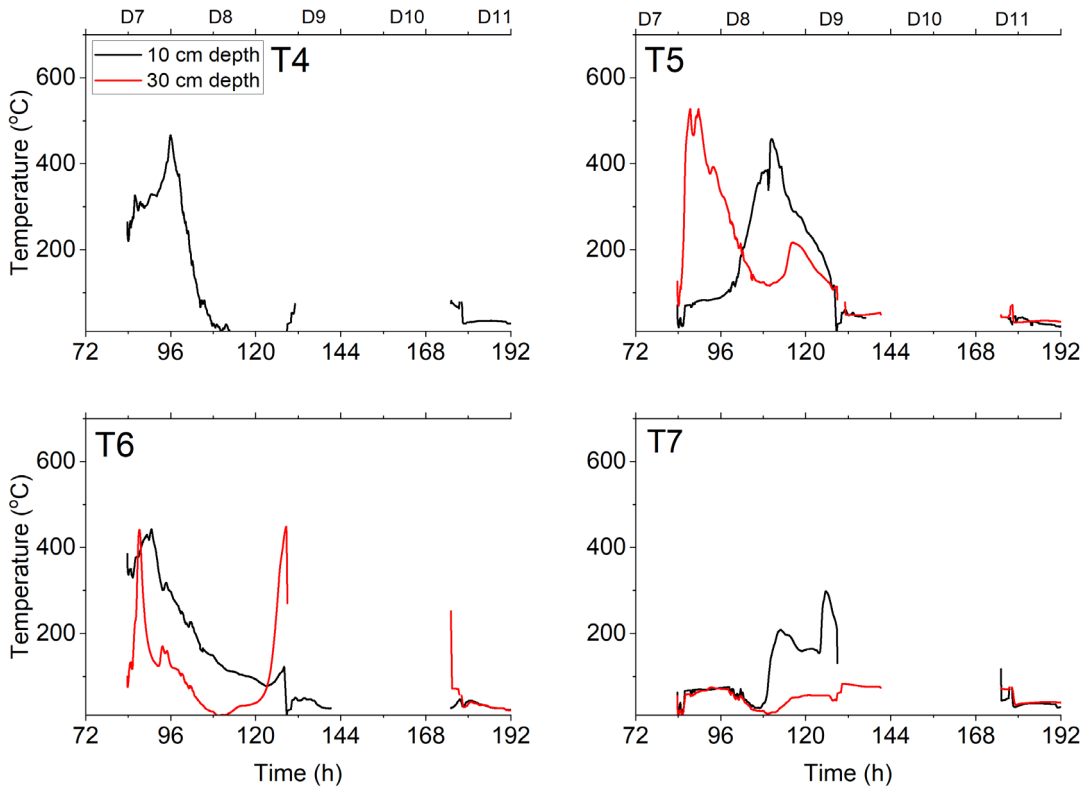

Figure A12. Temperature profiles in P3S fire showing all temperature measurement points as shown in Figure A6B. Time at 72 h indicates 00:00:00 am on day 7 (D7). Day is abbreviated to 'D' in this figure. Embers ignition was conducted on day 4 (D4) at ~09:27:00.

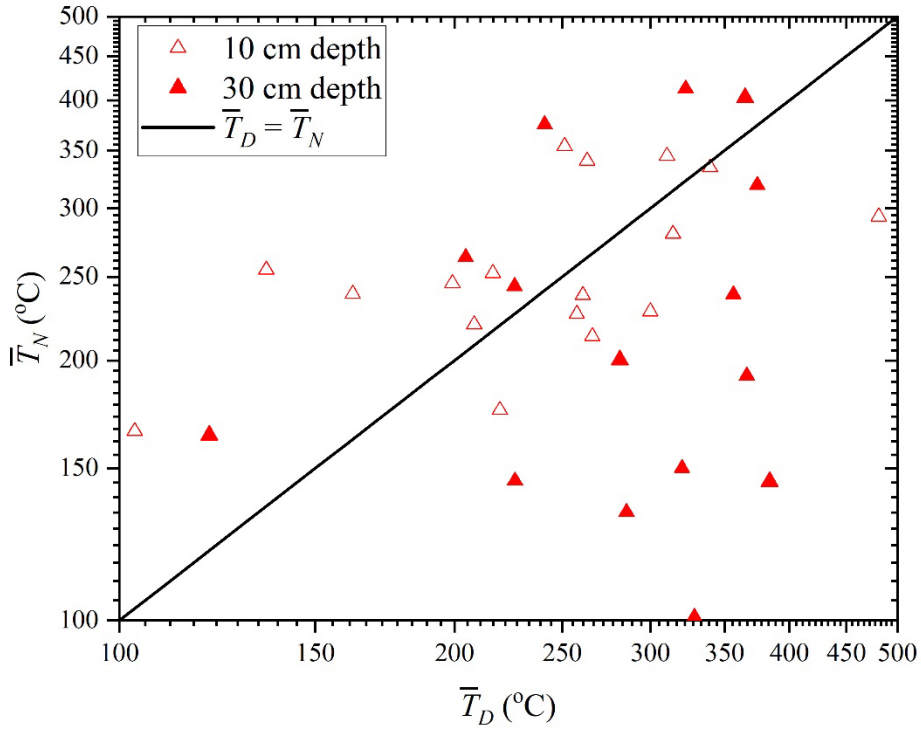

Figure A13. Smouldering thermal behaviour during day and night represented by average temperature. Each data point represents a thermocouple measurement point. Subscripts D and N refers to daytime and night-time, respectively.

Table A1. Location and number of measurements of Emission Factors of CO_2, CO, CH_4, NH_3, and HCN at each experiment stages. Each measurement was taken over 10 to 110 min.

Experiment stages	Measurement location (n= number of data)				
	CO_2	CO	CH_4	NH_3	HCN
Embers ignition	P1S (n=6)	P1S (n=6)	P1S (n=5)	P1S (n=4)	P1S (n=4)
Slash-and-burn ignition	P1N (n=1)	P1N (n=1)	P1N (n=1)	P1N (n=1)	P1N (n=1)
	P2N (n=1)	P2N (n=1)	P2N (n=1)	P2N (n=1)	P2N (n=1)
	P3N (n=2)	P3N (n=2)	P3N (n=2)	P3N (n=2)	P3N (n=2)
Smouldering spread	P1S (n=16)	P1S (n=16)	P1S (n=16)	P1S (n=16)	P1S (n=16)
	P1N (n=11)	P1N (n=11)	P1N (n=11)	P1N (n=11)	P1N (n=11)
Suppression	P1S (n=1)	P1S (n=1)	P1S (n=1)	P1S (n=1)	P1S (n=1)
	P1N (n=1)	P1N (n=1)	N/A	N/A	N/A
	P2N (n=1)	P2N (n=1)	P2N (n=1)	P2N (n=1)	P2N (n=1)

Table A2. Suppression method, flow rate ($\dot{V}_s$ (L/h)), fire area (A_f (m^2)), water spray or injection lance coverage area (A_s (m^2)), and suppression duration (Δt_s (h)) during the controlled suppression attempts conducted on day 11.

Fire location	Suppression method	$\dot{V}_s$ (L/h)	A_f (m^2)	A_s (m^2)	Δt_s (h)
P1N	Water spray	3024 ± 18	~80	30 ± 0.3	0.7 ± 0.2
P2N	Water spray	3024 ± 18	~20	30 ± 0.3	0.3 ± 0.03
P3S	Water spray	4878 ± 120	0.8	54 ± 1.5	0.4 ± 0.2
Pit 2 of P1S	Lance injection	1669	0.5	Point location	15 ± 1
Pit 3 of P1S	Lance injection	1669	0.3	Point location	13 ± 1

Equation A1. Besides suppression duration, the efficacy of suppression can also be expressed by water column height (H_s, mm). It represents the flux of the water over a fire area. H_s is calculated with Eq. A1 below, where $\dot{V}_s$ is the water flow rate (L h^{-1}), Δt_s is the suppression duration (h), A_f is the fire area (m^2), and A_s is the coverage area of the suppression method (m^2). Values for these variables are shown in Table A2 above. Since lance injection suppresses hot spots, the suppression was conducted with the aid of an infrared camera to detect a local hot spot at which point the lance was injected. As soon as the hotspots were not visible in the IR and temperatures were below 50°C, the suppression was considered successful and stopped.

$$H_s = \frac{\dot{V}_s \Delta t_s}{max(A_f, A_s)} \quad \text{(A1)}$$